Theoretical Model of High-Speed Tracked Vehicle General Motion

Stefan V. Milićević
PhD Student
University of Belgrade
Faculty of Mechanical Engineering

Ivan A. Blagojević
Full Professor
University of Belgrade
Faculty of Mechanical Engineering

This paper presents a systematically derived theoretical model for the motion of tracked vehicles, encompassing various scenarios such as soft terrain and slopes. The model considers all the resistances encountered by tracked vehicles, including track-terrain interaction, grade and air resistance, centrifugal force, inertial forces, and turning resistance. The heading angle determines the geometrical orientation of the vehicle on the slope. A MATLAB model of tracked vehicle general motion was established based on theoretical discussions. The paper discusses the steering performance of tracked vehicles on slopes of different inclinations. A simulation of steering with different turning radiuses was also presented. It is shown that the proposed model can be used for predicting and evaluating the steering performance of tracked vehicles with adequate accuracy. Furthermore, due to its high computational efficiency, the proposed model can be utilized for power demand modeling in research on the hybridization or electrification of tracked vehicles.

Keywords: *skid-steering, tracked vehicle, mathematical modeling, track-terrain interaction.*

1. INTRODUCTION

Tracked vehicles have a wide application ranging from construction and agriculture to military and mining. Steering of a tracked vehicle can be done using various methods, such as curved track steering and articulated steering, but the most widespread and notable is skid-steering. In skid-steering, the turning motion of the tracked vehicle is performed by achieving a difference in the speed of the inner and outer track. In this way, steering affects traction performance, i.e., forces on tracks, resultant resisting force, and the moment of the turning resistance.

Many studies on the mobility of tracked vehicles have been performed so far. The initial research on steering characteristics was presented by Steeds [1], who clarified the skid-steering mechanism, derived equations of motion, and set a foundation for subsequent studies on this topic, but made an assumption that the forces generated between the tracks and terrain obey the Coulomb law of friction which turned out incorrect. Bekker [2] established a connection between pressure and sinkage using the bevameter technique. Later on, relaying on Bekker's work, an empirical relation establishing the shear stress – shear displacement relationship was derived [3]. Using this relationship, a general theory for steady-state skid-steering on firm ground was established [4]. Using the general theory, the lateral coefficient of friction can be quantitatively determined as a function of the turning radius without the need for the use of empirical relations. Transient skid-steering models were developed relying on general theory [5,6]. In these papers, equations for track slip were derived for discretized tracks and numerically integrated to obtain track forces for vehicles on firm ground.

However, to the best of author's knowledge, only research that has studied lateral and longitudinal dynamics of tracked vehicles on slopes [7] deals with steering of articulated tracked vehicle and, as such, is very complex. Also, most other flat terrain skid-steering models are very complex, some of which deal with track tension and wheel-track interaction besides track-terrain interaction [8]. Numerical calculation of such models is computationally very burdensome. Different simplifi–cations are presented in the literature, e.g., introducing imaginary wheels and eliminating track chain [9], considering steady-state turns only [10], or appro–ximating the multibody model with single body model [11], but these skid-steering models remained computa–tionally demanding.

While hybrid propulsion systems have been very common in wheeled vehicles for many years [12], only recently has the hybridization of tracked vehicles gained interest [13-15]. With this increased interest in the hybridization and electrification of tracked vehicles and emerging autonomous tracked mobile robots, the need for computationally inexpensive yet high-fidelity skid-steering models is increasing. Many researchers create their own models with the goal of analyzing the impact of hybridization on fuel consumption. Since tracked vehicles operate over a variety of terrains, for such models, it is crucial to include all aspects of tracked vehicle movement, including traveling over a slope and soft terrain, while being computationally efficient for long and repetitive simulations. The motivation for this work stems from the mentioned fact and the general lack of research on all-round models encompassing all terrain conditions while being computationally inex–pensive.

This paper aims to derive general motion equations that would be efficient, simple, and applicable to all

Received: June 2023, Accepted: July 2023
Correspondence to: Stefan V. Milićević
Faculty of Mechanical Engineering,
Kraljice Marije 16, 11120 Belgrade 35, Serbia
E-mail: stefanm9670@gmail.com
doi: 10.5937/fme2303449M

driving conditions, including skid-steering on a slope, which hasn't been well presented in the literature.

2. BASICS OF TERRAMECHANICS

For the purpose of determining the shear stresses in the zone of track-terrain interaction, the shear stress-shear displacement relationship is used. Regardless of the size of the displacement, the size of the shear stress is a finite value and has its maximum, which is determined by the Mohr-Coulomb law, more often called just Coulomb's law, which states:

$$\tau_{\max} = c + \sigma \tan\phi \tag{1}$$

where τ_{max} is the maximum shear stress, c is the terrain cohesion, σ is the normal stress, and ϕ is the angle of internal shearing resistance.

Coulomb law implies that the maximum shear stress will be reached instantaneously as soon as the smallest relative movement happens. However, experimental data have shown that this is not the case. In reality, the maximum shear stress will be reached when the displacement reaches a certain value, as shown in Fig. 1.

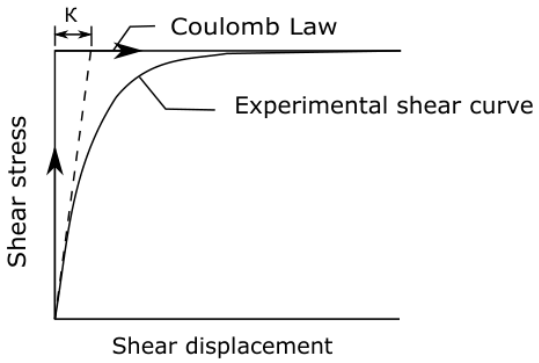

Figure 1. Comparison of theoretical and experimental shear stress-shear displacement relation

Therefore, the empirical relation widely used today was defined as:

$$\tau = \tau_{\max}\left(1 - e^{-\frac{j}{K}}\right) \tag{2}$$

where j is the shear displacement, and K is the shear deformation modulus.

The shear stress-shear displacement relationship also has its vertical counterpart called the pressure-sinkage relationship. The most commonly used equation has the following form [2]:

$$p = \left(\frac{k_c}{b} + k_\phi\right) z_0^n \tag{3}$$

where z_0 is the sinkage, p is the pressure, b is the cone radius, and n, $k_\square$, and k_c are pressure-sinkage parameters.

2.1 Resistances caused by track-terrain interaction

Resistance to motion due to track-terrain interaction includes three types of resistances:

- rolling resistance,
- compaction resistance and
- bulldozing resistance.

Rolling resistance can be expressed:

$$R_r = f_r \cdot Q \tag{4}$$

where Q is the ground normal reaction, and f_r is the rolling resistance coefficient defined as [16]:

$$f_r = f_0 + f_s V \tag{5}$$

where f_0 and f_s are empirical coefficients that depend on the design of tracks, and V is the vehicle speed.

The other two components are based on the estab–lished pressure-sinkage relationship. If (3) is written as:

$$z_0 = \left(\frac{p}{\frac{k_c}{b} + k_\phi}\right)^{\frac{1}{n}} \tag{6}$$

and assuming that track links are analogous to penet–rating bevameter and that pressure is uniformly distributed, this equation can be written down as:

$$z_0 = \left(\frac{\frac{G}{b \cdot l}}{\frac{k_c}{b} + k_\phi}\right)^{\frac{1}{n}} \tag{1}$$

where b and l are the width and length of the track contact surface. By integrating the pressure over depth, the work done to compact the soil is obtained:

$$W = b \cdot l \int_0^{z_0} p\,dz = b \cdot l \int_0^{z_0} \left(\frac{k_c}{b} + k_\phi\right) z_0^n\,dz \tag{8}$$

This equation combined with (6) gives:

$$W = \frac{b \cdot l}{(n+1) \cdot \left(\frac{k_c}{b} + k_\phi\right)} \left(\frac{G}{b \cdot l}\right)^{\frac{n+1}{n}} \tag{9}$$

If the work from (9) is represented as the product of the traction force and the length of the track's contact surface, the traction force will equal the resistance force due to the terrain compaction due to the sinking. Therefore, the resistance due to compaction can be expressed as:

$$R_c = \frac{1}{(n+1) \cdot b^{\frac{1}{n}} \cdot \left(\frac{k_c}{b} + k_\phi\right)^{\frac{1}{n}}} \left(\frac{G}{l}\right)^{\frac{1}{n}} \tag{10}$$

Bulldozing resistance occurs on deformable soil with significant sinkage. An accumulation of soil is for–med in front of the tracks, which acts as resistance to motion. This force is expressed as [17]:

$$R_b = b \cdot \left(c \cdot z_0 \cdot K_{pc} + 0.5 \cdot z_0^2 \cdot \gamma_s \cdot K_{p\gamma}\right) \tag{11}$$

where c is the terrain cohesion, γ_s is the specific weight of terrain, and K_{pc} and $K_{p\gamma}$ are terrain capacity factors.

Finally, total resistance due to the track-terrain interaction, i.e., the total road resistance, is obtained as:

$$R_m = R_r + R_c + R_b \tag{12}$$

3. LONGITUDINAL MOTION

Air resistance is often neglected in tracked vehicles due to low speeds. However, for high-speed vehicles with maximum movement speeds of over 60 km/h, air re–sistance significantly impacts total resistance. Air resistance is defined as:

$$R_{aero} = \frac{C_D \cdot \rho}{2} \cdot A \cdot V^2 \tag{13}$$

where C_D is the aerodynamic drag coefficient, ρ is the air density, and A is the vehicle frontal area.

In addition to air resistance, grade resistance can have a very large influence due to the large mass of tracked vehicles. Grade resistance is defined as:

$$R_{grade} = G \cdot \sin\alpha = mg \cdot \sin\alpha \tag{14}$$

where α is the road slope angle, when considering a turn on a slope, the grade resistance will be multiplied by a factor that takes into account the heading of the vehicle (heading angle), which defines the geometric orientation of the vehicle on the slope.

The vehicle's inertia and all rotating elements cause the appearance of inertial forces that oppose propulsive forces per the Lagrange-D'Alembert principle. The inertial force arising from the vehicle's mass is inherently included in the equation of motion. On the other hand, the inertial forces of the rotating elements in the kinematic connection with the sprocket wheels are not included. They can be modeled as special sub-models of transmission. Still, in vehicle dynamics theory studies, they are generally introduced together with translation inertial forces and, most often, through the mass coefficient[18].

$$R_a = \delta \cdot ma \tag{15}$$

where δ is the mass coefficient. An empirical formula related to tracked vehicles that define mass coefficient is proposed [19]:

$$\delta = 1.2 + 0.0025 \cdot i_{tr}^2 \tag{16}$$

where i_{tr} is the total transmission ratio.

Note that the previous calculation of inertial forces is simplified because it was assumed that there are no transmission losses and that there is only one power flow. For energy efficiency analysis, other models could be created.

4. LATERAL MOTION

The turning behavior of a tracked vehicle depends on the size of the propulsive forces of the outer F_0 and inner F_i track, the resultant resistance force R_{tot}, and the moment of turning resistance M_r created as a result of the soil's resistance to deformation. Along the entire contact surface of the tracks in the lateral direction, there are turning resistance forces that are proportional to the weight of the vehicle (Figure 2):

$$s = \mu \cdot \frac{G}{2 \cdot l} \tag{17}$$

where μ is the coefficient of lateral resistance which depends on the type of soil, design of the track chain, and turning radius.

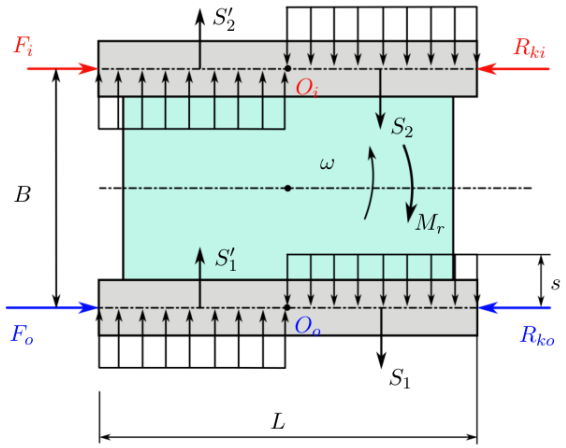

Figure 2. Forces acting on tracked vehicles during turning

The total moment of turning resistance is obtained as follows:

$$M_r = \mu \cdot \frac{G}{2 \cdot l} \int_0^{\frac{l}{2}} x dx = \mu \frac{G \cdot l}{4} \tag{18}$$

This equation is valid for *uniform* pressure distri–bution and *flat* terrain. Other cases will be derived in later text.

Coefficient of lateral resistance

Based on (17), it can be concluded that the coefficient of lateral resistance μ represents the proportionality coefficient between M_r and $Gl/4$, i.e., it is equivalent to the lateral coefficient of adhesion (friction). In the past, a constant value was often adopted for a certain type of base; however, constant values of the coefficient of resistance to turning did not give realistic solutions [20]. In this paper, an empirical formula will be used [21]:

$$\mu = \frac{\mu_{\max}}{a + (1-a) \cdot \left(\frac{R}{B} + \frac{1}{2} \right)} \tag{19}$$

where μ_{max} is the maximum μ at R = B/2, R is the theoretical turning radius, and a is the empirical coefficient (0,85 or 0,925 depending on the steering mechanism). Using (19), the coefficient of lateral resis–tance can be calculated for different values of the turning radius. Using the general theory and experi-mental data obtained from the literature [1,4], Figures 3 and 4 were created, which show a comparison of the proposed coefficient of lateral resistance to data obtained from the literature.

The proposed empirical formula achieves a high agreement with the experimental data. The general

theory gives a slightly higher degree of matching for greater speeds (Figure 4), but the mathematical model is significantly more complicated and computationally burdensome.

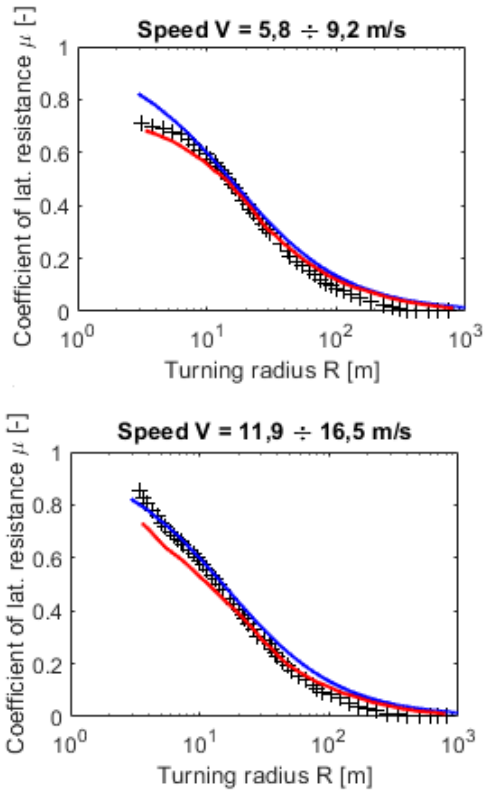

Figure 3. Comparison of coefficient of lateral resistance obtained with the proposed method, Wong's general theory, and experiment at lower speeds

4.2 Turning resistances

In the case of high-speed tracked vehicles, such as military-tracked vehicles, turning can be performed at very high speeds, and the centrifugal force cannot be ignored. Accordingly, the derivation of the mathematical model will be performed with the following assumptions:

- **The ground is firm** – consequently, compaction and bulldozing resistances in the lateral direction are negligible.
- **Pressure distribution is uniform** – assuming another pressure distribution (trapezoid, dual-trapezoid, etc.) is possible, but this results in an unnecessary complication of the mathematical model.
- **Centrifugal force is not negligible** and is taken into account – this assumption implies taking into account the centrifugal force, which can have a significant effect on the moment of turning resistance, especially at high speeds or very small turning radiuses.

Suppose that the tracked vehicle travels on the slope that forms angle α with the horizontal plane. When executing a turn, the vehicle changes the heading (direction) defined by the angle ψ = [0°, 360°]. The zero-heading angle is the initial movement heading along the slope, as shown in Figure 5. In addition to the already defined resistance forces, the vehicle is also affected by the centrifugal and weight forces. These components depend on the angle of slope and the angle of course. In accordance with the introduced assumptions, it is considered that the pressure distribution is always uniform.

By changing the heading angle ψ, the longitudinal and lateral components of the weight force appear, which are calculated as:

$$X = G \cdot \sin\alpha \sin\psi \, Y = G \cdot \sin\alpha \cos\psi \tag{20}$$

In the case of a turn, as illustrated in Figure 5, i.e., to the left (negative side) of the heading angle, the weight force components have directions as in Figure 6.

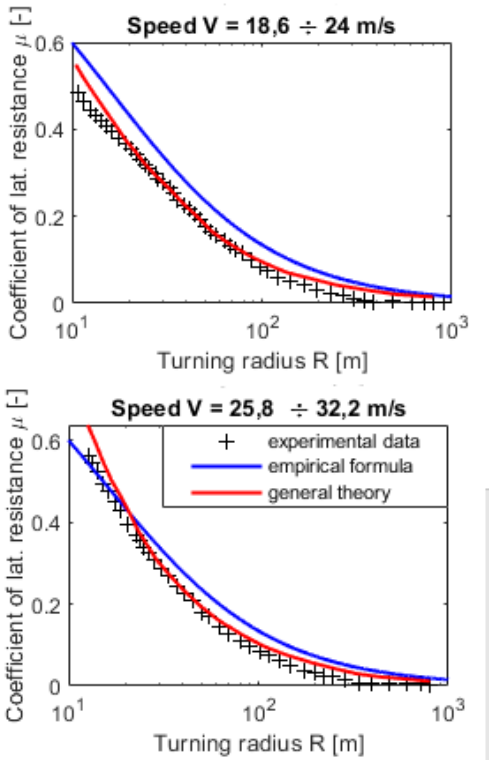

Figure 4. Comparison of coefficient of lateral resistance obtained with the proposed method, Wong's general theory, and experiment at higher speeds

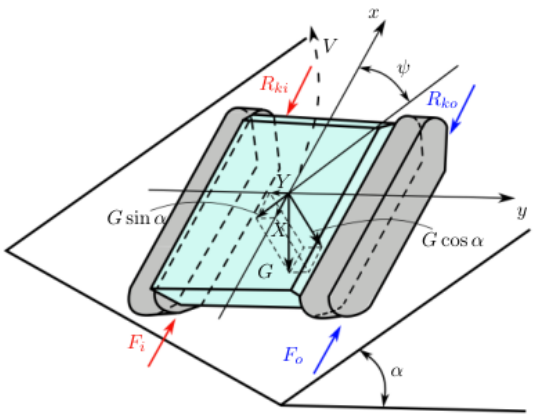

Figure 5. The general case of tracked vehicle motion on grade

Assuming uniform pressure distribution and constant μ along the entire length of tracks, in order to meet equilibrium conditions in the lateral direction, the sum of the turning resistance forces, the centrifugal force, and the lateral component of the weight force need to equal zero:

$$\left(\frac{l}{2}+s_0\right)\cdot\frac{\mu\cdot G\cos\alpha}{l}-\left(\frac{l}{2}-s_0\right)\cdot\frac{\mu\cdot G\cos\alpha}{l}+$$
$$+\frac{G\cdot V^2}{g\cdot R\cos\beta}-G\cdot\sin\alpha\sin\psi=0 \tag{21}$$

Since the turning radius R is usually significantly larger than contact length l, β can be approximated as $\cos\beta = 1$. After calculation and rearranging:

$$s_0=\frac{l}{2\cdot\mu\cos\alpha}\cdot\sin\alpha\sin\psi-\frac{l\cdot V^2}{2\cdot\mu\cos\alpha\cdot g\cdot R} \tag{22}$$

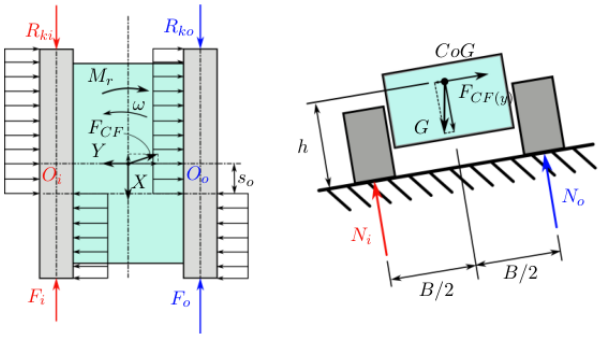

Figure 6. The general case of motion – back and top view

As a consequence of turn center offset, the corres–ponding moment of turning resistance has three compo–nents - the moment created by forces of turning resis–tance, the moment created by centrifugal force, and the moment created by the lateral component of the weight force:

$$M_r=\frac{\mu\cdot G\cos\alpha}{l}\left[\int_0^{\frac{l}{2}+s_0}x dx\int_0^{-\left(\frac{l}{2}-s_0\right)}x dx\right]+$$
$$+\frac{G\cdot V^2\cdot s_0}{g\cdot R}-g\cdot\sin\alpha\sin\psi\cdot s_0= \tag{23}$$
$$=\frac{\mu\cdot G\cos\alpha}{2\cdot l}\cdot\left(\frac{l^2}{2}+2\cdot s_0\right)+\frac{G\cdot V^2\cdot s_0}{g\cdot R}-G\cdot\sin\alpha\sin\psi\cdot s_0$$

Combining this equation with (22) gives:

$$M_r=\frac{\mu\cdot G\cos\alpha\cdot l}{4}\left[1-\left(\frac{\sin\alpha\sin\psi-\frac{V^2}{g\cdot R}}{\mu\cos\alpha}\right)^2\right] \tag{24}$$

When considering the transient motion, the moment of turning resistance needs to be reduced for rotational inertia factor $-I_z\cdot\varepsilon$ where I_z is the yaw moment of inertia, and ε is the angular acceleration.

5. GENERAL MOTION EQUATIONS

Generalizing the equations, i.e., assuming that the motion is carried out on soft terrain and at a variable speed, it is possible to derive general motion equations. The force on the outer and inner tracks are given as (25) and (26) on the bottom of the page spread out for clarity.

$$F_0=\left[\frac{G\cos\alpha}{2}+\frac{h}{b}\cdot\left(\frac{G\cdot V^2}{g\cdot R}-G\cdot\sin\alpha\sin\psi\right)\right]\cdot f_r+\frac{1}{2}\cdot\frac{1}{(n+1)\cdot b^{\frac{1}{n}}\cdot\left(\frac{k_c}{b}+k_\phi\right)^{\frac{1}{n}}}\left(\frac{G\cos\alpha}{1}\right)^{\frac{1}{n}}+\frac{b}{2}\cdot$$
$$\cdot\left(c\cdot\left(\frac{p}{\frac{k_c}{b}+k_\phi}\right)^{\frac{1}{n}}\cdot K_{pc}+0.5\cdot\left(\frac{p}{\frac{k_c}{b}+k_\phi}\right)\cdot\gamma_s\cdot K_{p\gamma}\right)+\frac{G\cdot V^2\cdot s_0}{2g\cdot R}+ \tag{25}$$
$$+\frac{G\cdot\sin\alpha\cos\psi}{2}+\frac{\delta mga}{2}+\frac{C_D\cdot\rho}{4}\cdot A\cdot V^2+\frac{\mu\cdot G\cos\alpha\cdot l}{4B}\cdot\left[1-\left(\frac{\sin\alpha\sin\psi-\frac{V^2}{g\cdot R}}{\mu\cos\alpha}\right)^2\right]$$

$$F_i=\left[\frac{G\cos\alpha}{2}-\frac{h}{b}\cdot\left(\frac{G\cdot V^2}{g\cdot R}-G\cdot\sin\alpha\sin\psi\right)\right]\cdot f_r+\frac{1}{2}\cdot\frac{1}{(n+1)\cdot b^{\frac{1}{n}}\cdot\left(\frac{k_c}{b}+k_\phi\right)^{\frac{1}{n}}}\left(\frac{G\cos\alpha}{1}\right)^{\frac{1}{n}}+\frac{b}{2}\cdot$$
$$\cdot\left(c\cdot\left(\frac{p}{\frac{k_c}{b}+k_\phi}\right)^{\frac{1}{n}}\cdot K_{pc}+0.5\cdot\left(\frac{p}{\frac{k_c}{b}+k_\phi}\right)\cdot\gamma_s\cdot K_{p\gamma}\right)+\frac{G\cdot V^2\cdot s_0}{2g\cdot R}+ \tag{26}$$
$$+\frac{G\cdot\sin\alpha\cos\psi}{2}+\frac{\delta mga}{2}+\frac{C_D\cdot\rho}{4}\cdot A\cdot V^2+\frac{\mu\cdot G\cos\alpha\cdot l}{4B}\cdot\left[1-\left(\frac{\sin\alpha\sin\psi-\frac{V^2}{g\cdot R}}{\mu\cos\alpha}\right)^2\right]$$

In equations (25) and (26), the first three terms on the right side represent the resistances arising from track-terrain interaction. Note that the normal reaction is modified due to the load transfer. The second and third terms do not depend on the slope of the terrain and the heading angle. The fourth and fifth terms are the longi–tudinal forces resulting from the effect of centrifugal force and the slope of the terrain, and the sixth and seventh terms are the acceleration and air resistance. The eighth term is the moment of turning resistance.

Derived equations enable describing the motion of a tracked vehicle in all possible conditions, including transient motion, deformable ground, and motion on a slope which, coupled with computational inexpensi–veness, makes these equations unique in the literature.

6. MODEL PERFORMANCE AND ANALYSIS

A general motion model was established in MATLAB based on the derived equations. A case of turning on the slope was considered in accordance with Figure 5. The tracked vehicle starts to turn from the reference position, i.e., from the straight uphill direction. Figure 7 and Figure 8 show forces on tracks during a 360-degree turn. The ground is assumed to be firm, the speed is constant, and the turning radius is constant and smaller than the free turning radius R_0 (Figure 10).

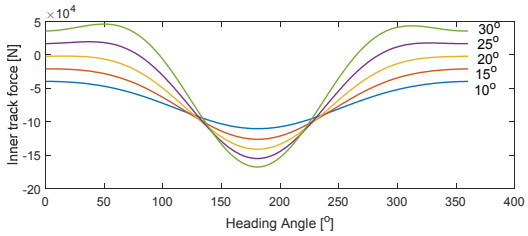

Figure 7. Inner track forces during turning on a slope

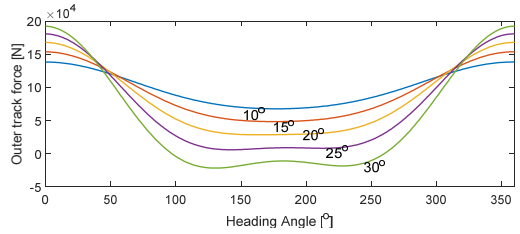

Figure 8. Outer track forces during turning on a slope

As shown in Figure 7 and Figure 8, when turning on a slope, the forces on the tracks change significantly. At the maximum slope angle of $\alpha = 30°$, both tracks exhibit braking forces in the range $\psi = [100°$ to $250°]$. Force on the inner track is negative for smaller α for the entire range of ψ which is in agreement with the vehicle dynamics theory, which states that at small R the force on the inner track is negative. For $\alpha > 20°$ force on inner track is positive for $\psi = [-70°, 70°]$ due to grade resistance force, which increases in intensity with α.

The decrease in force intensity when turning down a slope is due to the lateral force that creates a moment opposite to the moment of turning resistance, while the opposite case is present when turning upwards. A steering mechanism constructed with friction elements would not be able to achieve turns similar to the presented one due to the variability of the forces on the tracks. The sharpest rate of change of inner and outer track forces is exhibited in the range of $\psi = [100°$ to $250°]$ due to the vehicle's weight, namely its lateral component, which increases sharply in that range.

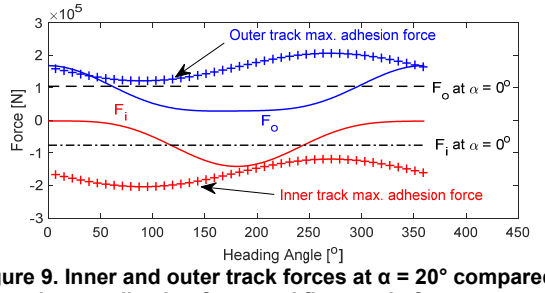

Figure 9. Inner and outer track forces at α = 20° compared to maximum adhesion force and flat terrain forces

The closer the heading angle is to $\psi = 180°$, the lower the force on the outer track, even becoming negative for very large slope angles. This happens due to the grade resistance force, which, with such orien–tation of the vehicle, acts as a propulsive force.

However, Figure 9 shows that at an angle of $\alpha = 20°$, slippage of the tracks is possible. With an increase in the slope angle, turning becomes impossible, which co–incides with empirical findings from the literature [21].

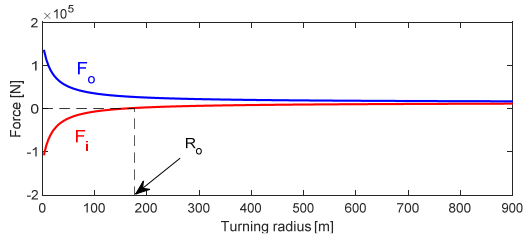

Figure 10.Inner and outer track forces at varying turning radiuses

When simulating a turn with different turning radiuses, forces on tracks change accordingly, as shown in Figure 10. Force on the outer track increases in intensity, while the force on the inner track decreases, and at radiuses smaller than free turning radius ($R < R_0$) becomes negative (braking force). This is due to the moment of turning resistance, or the coefficient of turning resistance, to be more specific. As the turning radius gets smaller, the moment of turning resistance increases in intensity, which causes the mentioned phenomenon.

7. CONCLUSION

This paper presents a systematically derived theoretical model for describing the motion of a tracked vehicle applicable to all possible conditions, including transient motion, soft terrain, and slopes. Special emphasis was given to modeling steering on slopes due to the existing research gap.

The theoretical model encompasses resistances arising from track-terrain interaction, grade and air resistance, resistance arising from centrifugal force, inertial forces, and moment of turning resistance. For the coefficient of lateral resistance, an empirical formula was used, the validity of which has been confirmed by comparison with experimental data from the literature and widely recognized Wong's general theory. The

heading angle determines the geometrical orientation of the vehicle on the slope.

A general motion model was established in MATLAB based on the derived equations. The steering performance of a tracked vehicle on the slope of varying inclination is discussed using the established model. It is shown that the proposed model can be used for predicting and evaluating the steering performance of tracked vehicles with adequate accuracy. Moreover, due to being computationally very efficient, the proposed model can be used for power demand modeling in research on the hybridization or electrification of trac–ked vehicles. By utilizing information about the soil's basic characteristics and the intended route of the vehi–cle, the required power can easily be determined. Such fast simulation will significantly reduce the time for drivetrain design iterations or the ability to implement online algorithms for power demand prediction.

Further work will focus on the unified modeling of hybrid and electric tracked vehicles and the creation of complete, scalable, and efficient models for analyzing and designing such vehicles.

REFERENCES

[1] Steeds, W.: Tracked vehicles, Automobile Engineer, Vol. 40, No. 4, 1950.

[2] Bekker, M. G.: *Theory of land locomotion*, University of Michigan Press, 1956.

[3] Janosi, Z. and Hanamoto, B.: *An analysis of the drawbar pull vs slip relationship for track laying vehicles*, Army tank-automotive center Warren MI, 1961.

[4] Wong, J.Y. and Chiang, C.F.: A general theory for skid steering of tracked vehicles on firm ground, Proceedings of the Institution of Mechanical Engineers, Pard D: Journal of Automobile Engineering, Vol. 215, No. 3, pp. 343-355, 2001.

[5] Ozdemir, M.N., Kilic, V. and Unlusoy, S.: A new contact & slip model for tracked vehicle transient dynamics on hard ground, Journal of terramechanics, Vol. 73, pp. 3-23, 2017.

[6] Solis, J.M. and Longoria, R.G.: Modeling track-terrain interaction for transient robotic vehicle maneuvers, Journal of terramechanics, Vol. 45, No. 3, pp. 65-78, 2008.

[7] Dong, C., Cheng, K., Hu, K. and Hu, W.: Dynamic modelling study on the slope steering performance of articulated tracked vehicles, Advances in Mechanical Engineering, Vol. 9, No. 7, pp. 1-26, 2017.

[8] Ma, Z. D. and Perkins, N.C.: A track-wheel-terrain interaction model for dynamic simulation of tracked vehicles, Vehicle System Dynamics, Vol. 37, No. 6., pp. 401-421, 2002.

[9] Mahalingam, I. and Padmanabhan, C.: A novel alternate multibody model for the longitudinal and ride dynamics of a tracked vehicle, Vehicle System Dynamcs, Vol. 53, No. 3, pp. 433-457, 2021.

[10] Tang, S., Yuan, S., Hu, J., Li, X., Zhou, J. and Guo, J.: Modeling of steady-state performance of skid-steering for high speed tracked vehicles, Journal of terramechanics, Vol. 73, pp. 25-35, 2017.

[11] Edwin, P., Shankar, K. and Kannan, K.: Soft soil track interaction modelling in single rigid body tracked vehicle models, Journal of terramechanics, Vol. 77, pp. 1-14, 2018.

[12] Blagojević, I., Mitić, S., Stamenković, D., Popović, V.: The future (and the present) of motor vehicle propulsion systems, Thermal Science, Vol. 23, pp. -1727-1743, 2019.

[13] Zou, Y., Liu, T., Liu, D., and Sun, F.:Reinforcement learning-based real-time energy management for a hybrid tracked vehicle, Applied energy, Vol. 171, pp. 372-382, 2016.

[14] Wang, H., Huang, Y., Khajepour, A., and Song, Q.: Model predictive control-based energy management strategy for a series hybrid electric tracked vehicle, Applied Energy, Vol. 182, pp. 105-114, 2016.

[15] Milićević, S. V., Blagojević, I. A., and Muždeka, S. R.: Advanced rule-based energy management for better fuel economy of hybrid electric tracked vehicle, FME Transactions, Vol. 49, No. 3, pp. 711-718, 2021.

[16] Ogorkiewicz, R. M.: *Technology of Tanks: Volumes I and II,* Surrey: Jane's Information Group, 1991.

[17] Wong, J. Y.: *Theory of ground vehicles*, John Wiley & Sons, 2008.

[18] Gillespie, T.: *Fundamentals of vehicle dynamics*, SAE International, 2021.

[19] Zabavnikov, N.A.: *Fundamentals of the theory of transport tracked vehicles*, Mashinostroenie, 1975. (in Russian)

[20] Kar, M. K.: Prediction of track forces in skid-steering of military tracked vehicles, Journal of Terramechanics, Vol. 24, No. 1, pp. 75-84, 1987.

[21] Nikitin, A.O. and Sergeev, L.V.: *Tank theory*, Publishing House of the Academy of Armored Forces, 1962. (in Russian)

NOMENCLATURE

τ_{max}	maximum shear stress
c	terrain cohesion
σ	normal stress
Φ	angle of internal shearing resistance.
J	shear displacement
K	shear deformation modulus
z_0	sinkage
p	pressure
l	track contact surface
b	bevameter (track pad) width
n, $k_\square$, k_c	pressure-sinkage parameters
Q	ground normal reaction
f_r	rolling resistance coefficient
f_0, f_s	empirical coefficients
V	vehicle speed.
γ_s	the specific weight of terrain
K_{pc}, $K_{p\gamma}$	terrain capacity factors
C_D	aerodynamic drag coefficient

P	air density
A	vehicle frontal area
α	road slope angle
δ	mass coefficient
i_{tr}	total transmission ratio
μ	coefficient of lateral resistance
R	theoretical turning radius
B	track contact width
a	empirical coefficient
Ψ	heading angle
M_r	moment of turning resistance
I_z	yaw moment
ε	angular acceleration
W	work done compacting soil
R_c	compaction resistance
R_b	bulldozing resistance
R_r	rolling resistance
R_m	total road resistance
R_{aero}	air resistance
R_{grade}	grade resistance
R_a	acceleration resistance
s_0	turn center offset
F_0	outer track force
F_i	inner track force

ТЕОРИЈСКИ МОДЕЛ ОПШТЕГ СЛУЧАЈА КРЕТАЊА БРЗОХОДНИХ ГУСЕНИЧНИХ ВОЗИЛА

С.В. Милићевић, И.А. Благојевић

У овом раду је презентован систематски изведен теоријски модел за кретање гусеничних возила, који обухвата различите случајеве као што су деформа–билни терен и нагиби. Модел узима у обзир све отпоре са којима се сусрећу гусенична возила, укљу–чујући отпоре услед интеракције гусеница-подлога, успон и отпор ваздуха, центрифугалну силу, инерци–јалне силе и отпор заокрету. Геометријска оријен–тација возила на нагибу одређује се углом курса. На основу теоријских разматрања, развијен је MATLAB модел општег кретања гусе–ничног возила. У раду се разматрају перформансе управљања гусеничних во–зила на успону различитог угла нагиба. Поред тога, приказане су и симулације управљања при разли–читим радијусима заокрета. Показано је да предло–жени модел може бити коришћен за предвиђање и оцењивање перформанси управљања гусеничних возила са одговарајућом прецизношћу. Додатно, због своје високе рачунске ефикасности, предло–жени модел се може корис–тити за моделирање потрошње енергије при истраживању хибридизације или електрификације гусеничних возила.